

Fate of quantum shock waves at late times

Thomas Veness and Leonid I. Glazman

Department of Physics, Yale University, New Haven, Connecticut 06520, USA



(Received 6 September 2019; published 17 December 2019)

Shock waves are a ubiquitous feature of hydrodynamic theories. Given that fermionic quantum many-body systems admit hydrodynamical descriptions on length scales large compared to the Fermi wavelength, it is natural to ask what the status of shock waves is in such systems. Free fermions provide a solvable yet nontrivial example, and here we generalize to include generic (nonintegrable) weak interactions to understand how a shock wave decays and changes its shape well after forming.

DOI: [10.1103/PhysRevB.100.235125](https://doi.org/10.1103/PhysRevB.100.235125)

I. INTRODUCTION

The notion of shock waves is well established in classical hydrodynamics [1]. If the fluid velocity is an increasing function of density, then any smooth density profile with a local maximum will eventually form a shock wave: a physical quantity becomes nonanalytic as a function of spatial coordinates. In fermionic systems, there is a tension between this singular behavior and the dispersive broadening one may expect at the level of single-particle quantum mechanics.

The nature of shock waves in the context of free fermions has been the subject of previous theoretical investigation [2–6]. In a particular classical limit, the formation of a shock wave is exhibited as a nonanalyticity in the density $\rho(x)$. Semiclassical corrections modify this by smoothing out the behavior at the shock front through the introduction of quantum ripples. It should be emphasized that prior work has focused on times close to the formation of the shock, where the ripples may be significant across the entirety of the structure associated with the shock. In Sec. II, we recapitulate these results and observe that for times well after shock formation a parametrically large spatial region has only negligible quantum corrections to the density.

Recently, the topic of generalized hydrodynamics [7–10] has led to significant progress in understanding the dynamics of quantities such as the density for integrable systems. The consequences of generic (i.e., nonintegrable) interactions are not clear from this picture, however. In this paper we linearize a Boltzmann equation and use single-particle decay rates to describe the effect of interactions. This technique allows us to investigate the shock wave at all spatial scales, excluding only a small spatial region affected by quantum corrections, and is valid for times well beyond that of shock formation.

The kinetic theory developed in Sec. III allows us to find the deformation of the spatial distribution of the density caused by relaxation. Despite the exponential decay of the number of fermions forming the shock wave, a substantial section of the shock wave retains its profile.

We present the final conclusions in Sec. IV, where we associate the dissolution of the shock wave with the interplay between the quantum-mechanical dispersion and the quasiparticle kinetics.

II. SHOCK WAVES FOR FREE FERMIONS

In order to present a self-contained discussion, we begin by recapitulating and extending some results from Ref. [6]. The question we wish to address is the following: for a system of spinless fermions, given an initial density profile

$$\rho(x) = \frac{k^0}{\pi} + \frac{k^m - k^0}{\pi} f\left(\frac{x}{w}\right), \quad (1)$$

how does the density evolve as a function of time? In Eq. (1), k^0/π is a background density corresponding to a uniform Fermi sea, and $(k^m - k^0)/\pi$ is the height of an isolated, smooth perturbation with profile $f(s)$. This has a single maximum at $f(0) \sim 1$ and $\lim_{|s| \rightarrow \infty} f(s) = 0$, varying on the scale $s \sim 1$ (the perturbation is of extent $\sim w$). We restrict to the scenario where the height of the perturbation is small $k^m - k^0 \ll k^0$, and the number of particles contained in the perturbation is large $\Delta N \sim (k^m - k^0)w \gg 1$. ΔN will be our large parameter for a semiclassical treatment.

The small height of the perturbation implies that excitations are confined to be particles and holes in the vicinity of the Fermi points. This gives us a well-defined notion of right and left movers. We initially consider the case of free fermions with a parabolic dispersion relation and mass m as given by the Hamiltonian

$$H = \sum_p \frac{p^2}{2m} \psi_p^\dagger \psi_p, \quad (2)$$

where ψ_p^\dagger and ψ_p are fermionic creation/annihilation operators at momentum p and obey the standard anticommutation relations, and we set $\hbar = 1$ throughout.

We are interested in a semiclassical description of the problem, and so introduce the Wigner function, defined by

$$\begin{aligned} W(x, k, t) &\equiv \int dy e^{-iky} \times \langle \Psi | e^{iHt} \psi^\dagger\left(x - \frac{y}{2}\right) \psi\left(x + \frac{y}{2}\right) e^{-iHt} | \Psi \rangle, \end{aligned} \quad (3)$$

where $|\Psi\rangle$ is the initial state at $t = 0$. The Wigner function is useful for a number of reasons: it allows us to perform a controlled semiclassical approximation with large parameter

ΔN , it provides simple access to the density, given by

$$\rho(x, t) = \int \frac{dk}{2\pi} W(x, k, t), \quad (4)$$

and finally, for H given by Eq. (2), $W(x, k, t)$ obeys the simple linear differential equation

$$\left(\partial_t + \frac{k}{m} \partial_x \right) W(x, k, t) = 0. \quad (5)$$

This results in the time-evolved Wigner function having the form $W(x, k, t) = W(x - kt/m, k, 0)$.

A. Classical picture

It is a natural ansatz that, due to the smooth variation of the density on the scale of the Fermi wavelength, the Wigner function of Eq. (3) may be described by a ‘‘local Fermi surface,’’ i.e.,

$$W_0(x, k, 0) \equiv \theta[k_F(x) - k] \theta[k_F(x) + k]. \quad (6)$$

Right and left movers separate on a timescale $t_{LR} \sim \frac{mw}{k^0}$. We therefore choose to ignore left movers with no loss of generality, and simplify the above to

$$W_0(x, k, 0) \approx \theta[k_F(x) - k] \theta(k^0 + k). \quad (7)$$

This leads to the implicit equation

$$k_F(x, t) = k_F[x - k_F(x, t)t/m, 0], \quad (8)$$

which gives rise to multivalued solutions on a timescale $t_S \sim \frac{mw}{k^m - k^0}$. This is consistent with ignoring left movers, as $t_{LR} \ll t_S$. The region where $k_F(x, t)$ is multivalued exists between the front of the shock, which we denote $x_+(t)$; and the back of the shock $x_-(t)$. Formally, $x_{\pm}(t)$ are the two solutions of $\partial_k x_F(k, t) = 0$ where $x_F(k, t)$ satisfies $k_F(x_F(k, t), t) = k$. At $t = t_S$ these two solutions coincide. For $t - t_S \ll t_S$, $x_+(t) - x_-(t) \sim w \left(\frac{t - t_S}{t_S} \right)^2$. For $t \gg t_S$ the difference between them (i.e., the extent of the shock) grows linearly in time as $x_+(t) - x_-(t) \sim (k^m - k^0)t$.

Between the points $x_-(t)$ and $x_+(t)$, $k_F(x, t)$ has three branches which we will denote $k_F^{(0)}(x, t) \leq k_-(x, t) \leq k_+(x, t)$. It is evident from Fig. 1 that near $x_+(t)$ the density acquires square-root behavior in $x_+(t) - x$, and so within the ansatz of Eq. (7) a nonanalyticity in the density arises.

B. Semiclassical corrections

The main result of Ref. [6] is to quantify how, for a specific form of initial state $|\Psi\rangle$, including the leading semiclassical correction rounds off the nonanalytic behavior. We begin from the same point, specifying the initial state as

$$|\Psi\rangle = e^{i \int dx \rho^R(x) \Phi(x)} |0\rangle. \quad (9)$$

Here, $\rho^R(x)$ is the density associated with right movers, $|0\rangle$ is the (translationally invariant) ground state with Fermi momentum k^0 , and $\Phi(x)$ is a smooth function corresponding to a density $\rho(x) = k^0/\pi + \Phi'(x)/(2\pi)$, i.e., $\Phi'(x) \leftrightarrow k_F(x) - k^0$. This state has convenient analytic structure, and is experimentally relevant in terms of being preparable by a sudden large perturbation [4, 11].

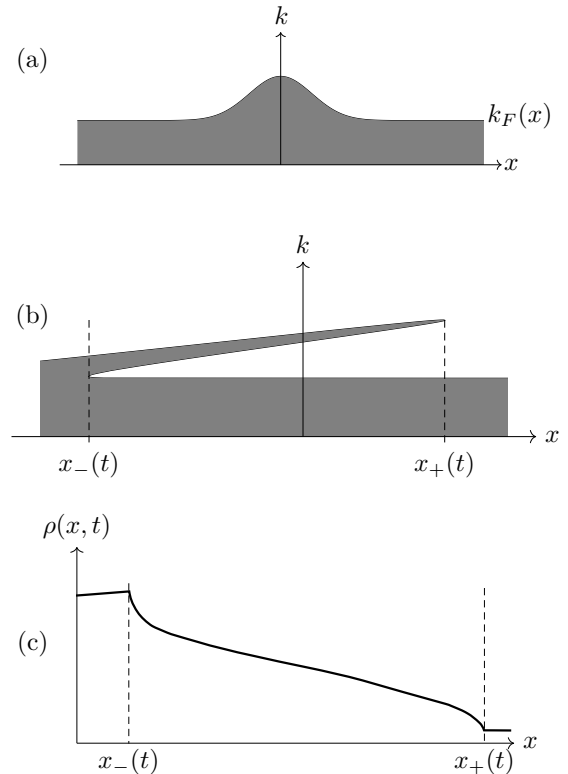


FIG. 1. Schematic for free fermions in the classical limit $\Delta N \rightarrow \infty$, showing (a) the Wigner function for $k > 0$ and $t = 0$, where in the shaded region the Wigner function is 1, and vanishes elsewhere; (b) the Wigner function for $k > 0$ and $t > t_S$: the shock wave has now formed between $x_-(t)$ and $x_+(t)$; (c) the density $\rho(x, t)$ corresponding to $t > t_S$, given by integrating (b) in the k direction as in Eq. (4). Due to taking the classical limit, nonanalytic behavior is observed at $x_-(t)$ and $x_+(t)$.

Considering only right movers, standard bosonization techniques give an explicit integral representation for the Wigner function at $t = 0$ of

$$W(x, k, 0) = \int dy e^{i(k^0 - k)y} \frac{e^{i[\Phi(x+y/2) - \Phi(x-y/2)]}}{2\pi i(y + i0^+)}. \quad (10)$$

Performing a gradient expansion of Φ in the exponent, it is clear that retaining only the linear-in- y term leads to the step-function approximation of Eq. (7). This approximation is justified in the $\Delta N \rightarrow \infty$ limit, where the ansatz of Eq. (7) as describing Eq. (3) is exact. Keeping the y^3 term in Eq. (10) amounts to including semiclassical corrections. The excess density may be expressed in terms of the distance from the front of the shock as

$$\begin{aligned} \frac{\delta \rho(x, t)}{k^m - k^0} &\equiv \frac{\langle \Psi | \rho(x, t) | \Psi \rangle - \langle 0 | \rho(x, t) | 0 \rangle}{k^m - k^0} \\ &= \frac{t_S}{t \Delta N^{1/3}} \left[\text{Ai}' \left(\frac{x_+(t) - x}{\ell(t)} \right)^2 \right. \\ &\quad \left. - \frac{x_+(t) - x}{\ell(t)} \text{Ai}^2 \left(\frac{x_+(t) - x}{\ell(t)} \right) \right], \quad (11) \end{aligned}$$

where the length scale $\ell(t)$ is given by

$$\ell(t) = \left(\frac{\partial_k^2 x_F(k, t)|_{k_F(x_+(t), t)}}{2} \right)^{1/3} \sim \frac{1}{2^{1/3}(\Delta N)^{2/3}} \frac{t}{t_S} w, \quad (12)$$

and Ai is an Airy function [6]. Note that the previous work focused on times shortly after the formation of the classical shock ($t - t_S \ll t_S$, $x_+ - x_- \ll w$), and identified the small parameter $1/\Delta N^{2/3}$ required for the classical description to be valid. The main result of Ref. [6] is that the scaling function of Eq. (11) gives a good description of the ripples for the entire interval $x_+ - x_- \lesssim w$ until times $t - t_S \sim t_S$. In fact, as shown in Appendix A, Eq. (11) continues to give a good description at all times $t \gtrsim t_S$ for $x_+(t) - x \ll x_+(t) - x_-(t)$.

Because the extent of the shock grows linearly with time for $t \gg t_S$, it will be useful to introduce a dimensionless parameter measuring the distance from the front of the shock:

$$\lambda(x, t) \equiv \frac{x_+(t) - x}{x_+(t) - x_-(t)}. \quad (13)$$

In terms of this dimensionless variable, we may express the asymptote of Eq. (11) for $\lambda > 0$ as

$$\frac{\delta\rho[\lambda, t]}{(k^m - k^0)} \approx \frac{\sqrt{\lambda} t_S}{\pi t} \left(1 + \frac{\sin\left(\frac{2}{3}(\lambda/\lambda_{\text{cr}})^{3/2}\right)}{2\lambda/\lambda_{\text{cr}}} \right), \quad (14)$$

where the crossover scale $\lambda_{\text{cr}} = \frac{1}{(\Delta N)^{2/3}}$. For the regime $1 \gg \lambda \gg \lambda_{\text{cr}}$, semiclassical corrections are negligible and the simple step function of Eq. (7) captures the essential physics. In other words, although the spatial window where quantum corrections are appreciable grows with time, it is parametrically small on the length scale of the shock.

How this window changes over time can be understood simply: the length scale for quantum corrections $\ell(t)$ grows linearly in time. At times $t - t_S \ll t_S$, the extent of the shock is small as $x_+(t) - x_-(t) \sim w(t - t_S)^2/t_S^2$ and the quantum corrections are significant. However, at late times $t - t_S \gg t_S$, while the length scale $\ell(t)$ grows linearly in time, so too does the extent of the shock and we have that $\frac{x_+(t) - x_-(t)}{\ell(t)} \sim \Delta N^{2/3}$, i.e., the ripples are squeezed into a fraction $\Delta N^{-2/3}$ of the shock. Therefore, quantum corrections are most significant around the time $t = t_S$, when the shock nucleates. For $t - t_S \gg t_S$, the fraction of the shock smeared by quantum fluctuations λ_{cr} remains finite and independent of time.

We wish to add small, generically integrability-breaking interactions to this picture. Having established the regime within which semiclassical corrections are small, restricting to this will allow us to make further analytic progress.

III. ADDING GENERIC INTERACTIONS

We wish to understand how adding interactions changes the behavior at late times, restricting to small interactions such that the shock structure of free fermions can become established before decay processes start taking effect. Well after the formation of the overhanging profile of Fig. 1(b), particles above the Fermi surface will begin to relax toward lower energies. This modifies the Wigner function from the steplike behavior of Fig. 1, and it will generically be nonzero

for $k^0 < k < k_-(x, t)$ and $x_-(t) < x < x_+(t)$. We will examine how to modify the free-fermionic description to account for integrability-breaking interactions, and how this changes the evolution of the density as a function of time.

In one dimension, two-particle collisions do not redistribute energy and momentum. Generic interactions permit three-particle collisions, which leads to the relaxation of excited states [12]. We denote the decay rate for single-particle excitations over the Fermi sea with momentum $k > k^0$ by $\Gamma(k)$. We wish to incorporate this decay rate, with characteristic magnitude $\Gamma(k^m)$, into our description of the time evolution of the shock. By working explicitly in the regime where $\Gamma(k^m)t_S \ll 1$, the shock profile is established before decay processes become important. We also require $t \gg t_S$, $1 \gg \lambda \gg \lambda_{\text{cr}}$ such that we may dispense with ripples. Accordingly, one may view the Wigner function as the distribution function in the classical limit $f(x, k, t)$. In the absence of integrability, three-particle collisions lead to a redistribution of the occupied states, and this is captured by the kinetic (Boltzmann) equation [13,14]

$$\left(\partial_t + \frac{k}{m} \partial_x \right) f(x, k, t) = I\{f\}, \quad (15)$$

where I is a three-particle collision integral. In principle, the advective term is modified by renormalization of the dispersion due to interactions. For local interactions, corrections to the parabolic spectrum are suppressed by factors of $(k - k_F)/k_F$, which is small by assumption and may be neglected.

We wish to evaluate how the shock structure fades on times $t \gtrsim 1/\Gamma(k^m)$. At these long times, the variation of the spatial structure is smooth on the scale of the Fermi wavelength. Intuitively, interactions will lead to a decay of $f(x, k, t)$ at ‘‘high energies’’ [i.e., for k between $k_-(x, t)$ and $k_+(x, t)$], which will act as a source for ‘‘low energies’’ [k between k^0 and $k_-(x, t)$]. Linearizing the collision integral I gives an equation of the form

$$\left(\partial_t + \frac{k}{m} \partial_x \right) f(x, k, t) = J(x, k, t) - \Gamma(k)f(x, k, t). \quad (16)$$

Here, $J(x, k, t)$ represents ‘‘high-energy’’ particles decaying and acting as a source for $f(x, k, t)$, and $\Gamma(k)$ is the aggregate of decay processes from momentum k to lower energies. In terms of the decay rate from p to the interval $[k, k + \delta k]$, which we denote $\mathcal{W}_{p \rightarrow k} \delta k$, $J(x, k, t)$ and $\Gamma(k)$ are given by

$$J(x, k, t) = \int_k^{k_+(x, t)} dp f(x, p, t) \mathcal{W}_{p \rightarrow k},$$

$$\Gamma(k) = \int_{k^0}^k dp \mathcal{W}_{k \rightarrow p}. \quad (17)$$

Formally, Eq. (16) is a linear integrodifferential equation. We decompose $f(x, k, t)$ into ‘‘low-energy’’ [below $k_-(x, t)$] and ‘‘high-energy’’ [between $k_-(x, t)$ and $k_+(x, t)$] pieces:

$$f(x, k, t) = \begin{cases} f_{\text{low}}(x, k, t), & k^0 < k \leq k_- \\ f_{\text{high}}(x, k, t), & k_- < k \leq k_+. \end{cases} \quad (18)$$

If we focus on the region in k between $k_-(x, t)$ and $k_+(x, t)$, there is no source for particles: $J(x, k, t) = 0$ for $k_-(x, t) <$

$k < k_+(x, t)$. In the accepted approximation, $f_{\text{high}}(x, k, t)$ satisfies the equation

$$\left(\partial_t + \frac{k}{m}\partial_x\right)f_{\text{high}}(x, k, t) = -\Gamma(k)f_{\text{high}}(x, k, t). \quad (19)$$

The initial conditions are defined by the free evolution within the time frame $t_S \ll t \ll \frac{1}{\Gamma(k^m)}$. The corresponding solution of Eq. (19) is

$$f_{\text{high}}(x, k, t) = \theta[k - k_-(x, t)]\theta[k_+(x, t) - k]e^{-t\Gamma(k)}. \quad (20)$$

This is simply the result of Eq. (7) augmented with the finite lifetime of fermions above the Fermi surface. Immediately below this region, $k \lesssim k_-(x, t)$, the only contribution to the source term $J(x, k, t)$ in Eq. (16) comes from $f_{\text{high}}(x, k, t)$. It is therefore appropriate that Eq. (17) may be approximated by

$$\begin{aligned} J(x, k, t) &\approx \int_0^{k_+(x, t)} dp f_{\text{high}}(x, p, t)\mathcal{W}_{p \rightarrow k} \\ &= \int_{k_-(x, t)}^{k_+(x, t)} dp e^{-t\Gamma(p)}\mathcal{W}_{p \rightarrow k}. \end{aligned} \quad (21)$$

We will comment upon the consistency of this approximation at the end of this section. This approach means that $J(x, k, t)$ and $\Gamma(k)$ are independent of $f(x, k, t)$, and the solution of Eq. (16) for $k^0 < k < k_-(x, t)$ is easily verified as

$$f_{\text{low}}(x, k, t) = \int_0^t dt' e^{-(t-t')\Gamma(k)} J[x - k(t-t'), k, t']. \quad (22)$$

This corresponds to integrating over all contributions from modes which are sourced by the term J , and also allows for decay.

Concretely, we now consider a Hamiltonian of the form

$$H = \sum_p \frac{p^2}{2m} \psi_p^\dagger \psi_p + \frac{1}{2L} \sum_{\substack{q \neq 0 \\ \alpha = R, L}} (V_q \rho_q^\alpha \rho_{-q}^\alpha + 2U_q \rho_q^R \rho_q^L), \quad (23)$$

where $\rho_q^{R/L} = \sum_k \psi_{k-q}^{R/L\dagger} \psi_k^{R/L}$ is the Fourier component of the density operator for right and left movers, respectively. It is therefore sensible to consider $\mathcal{W}_{p \rightarrow k}$ [and accordingly $\Gamma(k)$] as that given by the single-particle decay rate of Ref. [15]. In terms of the decay rate $\Gamma(k^m)$ at k^m we can express

$$\begin{aligned} \mathcal{W}_{p \rightarrow k} &= c \frac{(k - k^0)^2 (p - k)^5}{(k^m - k^0)^8} \Gamma(k^m), \\ \frac{\Gamma(p)}{\Gamma(k^m)} &= \frac{(p - k^0)^8}{(k^m - k^0)^8}, \end{aligned} \quad (24)$$

with corrections suppressed by factors of $(p - k^0)/k^0 \ll 1$. Here, $c = 168$ is a normalization constant such that $\int_{k^0}^{k^m} dk \mathcal{W}_{k^m \rightarrow k} = \Gamma(k^m)$. In evaluating Eq. (21), we assume that $t \gg t_S \sqrt{\lambda}$, and may replace the exponential and the rate $\mathcal{W}_{p \rightarrow k}$ by their averages in the interval:

$$J(x, k, t) \approx [k_+(x, t) - k_-(x, t)] e^{-t\Gamma(\bar{k})} \mathcal{W}_{\bar{k} \rightarrow k}, \quad (25)$$

where $\bar{k} = \frac{1}{2}[k_+(x, t) + k_-(x, t)]$ and vanishes otherwise. To ease notation, we set $m = 1$ for the remainder of the paper.

Having dispensed with ripples, simple geometric considerations dictate that the integrand in Eq. (22) is only nonzero for

$$x - k(t - t') \leq x_+(t'), \quad (26)$$

which determines an inequality for t' in Eq. (22)

$$t' \geq t_1 \equiv \frac{x - kt}{k^m - k}, \quad (27)$$

and so we can rewrite it as

$$f_{\text{low}}(x, k, t) = \int_{t_1}^t dt' e^{-(t-t')\Gamma(k)} J[(k^m - k)t_1 + kt', k, t']. \quad (28)$$

Hereinafter, x should be understood as a function of λ and t . Using these new variables, we may use the explicit expression for \mathcal{W} given by Eq. (24) and discard subleading corrections in λ to find

$$\begin{aligned} f_{\text{low}}(x, k, t) &\approx 2c\Gamma(k^m)t_S \left(\frac{k^m - k}{k^m - k^0}\right)^{11/2} \left(\frac{k - k^0}{k^m - k^0}\right)^2 \\ &\times \int_{t_1}^t \frac{dt'}{t_1} \left(\frac{t_1}{t'}\right)^6 \sqrt{1 - \frac{t_1}{t'}} e^{-(t-t')\Gamma(k)} e^{-t'\Gamma(k^m)}. \end{aligned} \quad (29)$$

To determine the behavior of this integral, it is crucial to know the behavior of the exponential inside the integrand. To make this clearer, we introduce the dimensionless variable

$$\tau \equiv \frac{t' - t_1}{t_1}. \quad (30)$$

In terms of this, we may write

$$\begin{aligned} f_{\text{low}} &\approx 2c\Gamma(k^m)t_S e^{-(t-t_1)\Gamma(k) - t_1\Gamma(k^m)} \left(\frac{k^m - k}{k^m - k^0}\right)^{11/2} \\ &\times \left(\frac{k - k^0}{k^m - k^0}\right)^2 \int_0^{\frac{t-t_1}{t_1}} \frac{d\tau \sqrt{\tau}}{(1 + \tau)^{13/2}} e^{-t_1\tau[\Gamma(k^m) - \Gamma(k)]}. \end{aligned} \quad (31)$$

It will be helpful to also introduce a dimensionless variable γ which interpolates in the k direction between the overhanging tip ($\gamma = 0$) and the background Fermi sea ($\gamma = 1$), defined by

$$k - k^0 = (k^m - k^0)(1 - \lambda)(1 - \gamma). \quad (32)$$

Rewriting in terms of the variables λ, γ, t , the leading behavior of Eq. (28) may be approximated by

$$\begin{aligned} f_{\text{low}}[\lambda, \gamma, t] &\approx 2c\Gamma(k^m)t_S [\gamma + \lambda]^{11/2} (1 - \gamma)^2 e^{-t\Gamma(k^m)} \\ &\times \int_0^{\lambda/\gamma} d\tau \frac{\sqrt{\tau}}{(1 + \tau)^{13/2}} e^{-\tau\Gamma(k^m)\gamma}. \end{aligned} \quad (33)$$

The contribution to the density coming from the high-energy region, i.e., $k_-(x, t) < k < k_+(x, t)$, behaves as

$$\begin{aligned} \delta\rho_{\text{high}}[\lambda, t] &= \int_{k_-[\lambda, t]}^{k_+[\lambda, t]} \frac{dk}{2\pi} W(x, k, t) \\ &\approx (k^m - k^0) e^{-t\Gamma(k^m)} \frac{t_S \sqrt{\lambda}}{t\pi}. \end{aligned} \quad (34)$$

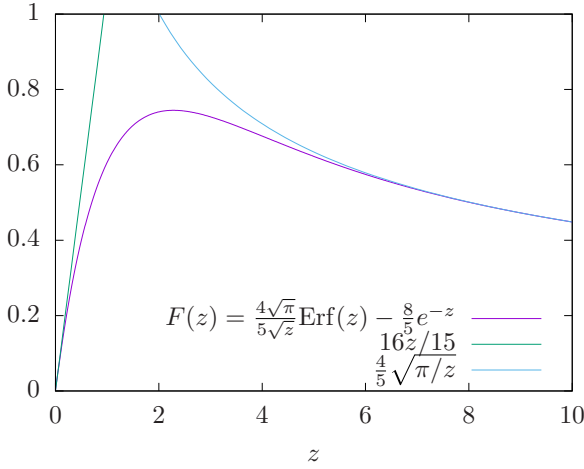


FIG. 2. Scaling function $F(z)$ of Eq. (36) describing correction to $\delta\rho_{\text{high}}$. The asymptotes of $F(z)$ are shown for $z \ll 1$, where the behavior is linear, and $z \gg 1$, where $F(z)$ falls off as $z^{-1/2}$.

The contribution to the density coming from the low-energy region is given by integrating Eq. (33) over $k^0 < k < k_-(x, t)$, which translates to

$$\delta\rho_{\text{low}} = \frac{(k^m - k^0)}{2\pi} \int_0^1 d\gamma f_{\text{low}}[\lambda, \gamma, t]. \quad (35)$$

Using Eq. (33) and noticing that the dominant contribution to $\delta\rho_{\text{low}}$ comes from $\gamma \sim \mathcal{O}(1)$, Eq. (35) may be evaluated to leading order in λ (see Appendix B), yielding

$$\delta\rho^{\text{low}}[\lambda, t] \approx F(\lambda t \Gamma(k^m)) \delta\rho_{\text{high}}[\lambda, t]. \quad (36)$$

Here, $\delta\rho_{\text{high}}$ is given by Eq. (34) and we have used the function

$$F(z) = \frac{8}{5\sqrt{z}} \int_0^z dy \sqrt{y} e^{-y}, \quad (37)$$

which is plotted in Fig. 2. We note that the form of $F(z)$ appears to be largely insensitive to the particular form of \mathcal{W} . This correction is maximal at $\lambda t \Gamma(k^m) \sim 1$. We have argued that the ballistic result of Eq. (34) is modified with a contribution from “lower energies,” giving

$$\delta\rho[\lambda, t] \approx (k^m - k^0) e^{-t\Gamma(k^m) \frac{t_S \sqrt{\lambda}}{t\pi}} [1 + F(\lambda t \Gamma(k^m))], \quad (38)$$

which remains a monotonic function of λ , as shown in Fig. 3. In dimensional variables the shock wave preserves its form away from the front over the time-independent scale $x_+(t) - x \sim \frac{w}{\Gamma(k^m)t_S}$, while the entire shock-wave structure (see Fig. 4) expands linearly in time as $x_+(t) - x_-(t) \sim w \frac{t}{t_S}$.

The behavior of quantum ripples in the presence of interactions is not addressed by our approach. The ripples of Sec. II arise from the quantum-mechanical dispersion of a single particle, and it is this dispersion that gives rise to the length scale $\ell(t) \sim (\Delta N)^{2/3} w t / t_S$ of Eq. (12). In writing the Boltzmann equation of Eq. (15), we coarse grain on a scale

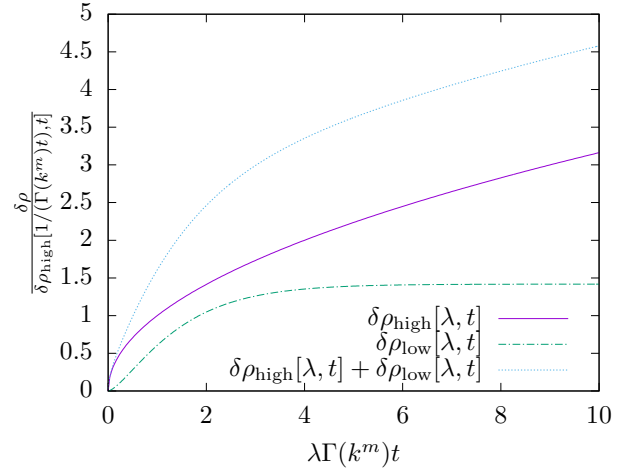


FIG. 3. Plot of the contributions to the shock-wave density $\delta\rho = \delta\rho_{\text{low}} + \delta\rho_{\text{high}}$ appearing in Eq. (38). The contribution coming from lower energies $\delta\rho_{\text{low}}$ is comparable to $\delta\rho_{\text{high}}$ when $\lambda t \Gamma(k^m) \sim 1$. The inelastic processes cause particles to decay to states with lower energies, which due to their slower velocity leads to an overall decay of the shock. This redistribution has a nonuniform momentum dependence and thus causes a nontrivial restructuring of the shock. $\delta\rho_{\text{high}}$ captures the part of the density coming from fermions which did not relax and propagated ballistically within the original shock-wave formation until time t .

larger than this quantum dispersion length. The Boltzmann equation is therefore appropriate only if the quantum dispersion length scale is much smaller than the coarse-grained one. As the former scale grows linearly in time, while the scale for variation of Eq. (38) is independent of time, the results of this section are applicable for times $t \lesssim (\Delta N)^{2/3} / \Gamma(k^m)$.

With our expression for f_{low} in Eq. (33), it is also possible to comment on the consistency of the assumption of the region $[k_-(x, t), k_+(x, t)]$ being the dominant contribution to $J(x, k, t)$, as asserted in Eq. (21). By evaluating the contribution to J for momenta below $k_-(x, t)$, as outlined in Appendix C, one finds that the relative correction is not asymptotically small for all times, with behavior similar to that of Eq. (36). However, the correction is in fact numerically small, on the order of 2% at the largest, and so the approximation of Eq. (21) appears to be consistent.

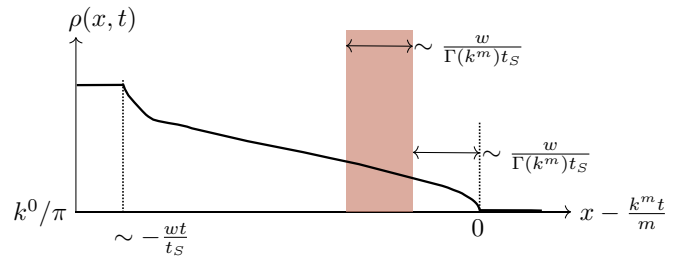


FIG. 4. Schematic of the density $\rho(x, t)$ as given by Eq. (38). The ballistic form of $\delta\rho_{\text{high}}$ in Eq. (34) is preserved on a scale $\sim w / \Gamma(k^m) t_S$ from the tip of the shock. There is a window of extent $\sim w / \Gamma(k^m) t_S$ where the contribution to $\delta\rho$ from $\delta\rho_{\text{low}}$ given by Eq. (36) is significant. The overall size of the shock structure grows as $w t / t_S$.

IV. CONCLUSIONS

For free fermions, introducing a density disturbance of width w containing $\Delta N \gg 1$ particles leads to the formation of a shock structure on a timescale which may be estimated from classical mechanics as $t_S \sim \frac{w^2}{\Delta N}$. Semiclassical corrections in the form of quantum ripples exist in a region of the front of the shock for all times. As quantified in Sec. II, the size of this region grows linearly with time, but with a parametrically small coefficient. In dimensionful variables, the quantum ripples occur on the scale $x_+(t) - x \sim \frac{wt}{t_S(\Delta N)^{2/3}}$. The fraction of the shock for which ripples are significant is given by $\lambda_{\text{cr}} \sim (\Delta N)^{-2/3}$, and so most of the shock is well described classically.

Using this reasoning to disregard ripples, one may now separately consider the effects of relaxation due to including interactions. Generic interactions lead to the decay of excitations high above the Fermi sea at the expense of creating a large number of low-energy excitations. These high-energy excitations have a characteristic decay rate $\Gamma(k^m)$. To establish continuity between the free and interacting pictures, we make the restriction that $t_S \Gamma(k^m) \ll 1$: the profile of the shock is manifestly unchanged for short times, as interactions have barely “turned on.” Decay processes are only pertinent at $t \Gamma(k^m) \gtrsim 1$, well after the shock has been established.

Our analysis of the linearized Boltzmann equation of Eq. (16) yields the behavior of the fermionic density at times $t \gg t_S$. For any time $t \gtrsim \Gamma(k^m)^{-1}$ the deviations from a simple exponentially decaying ballistic theory are given by the function $F(\lambda t \Gamma(k^m))$ in Eq. (38). This term is significant only for $\lambda \sim 1/[t \Gamma(k^m)]$. In dimensionful variables, the kinetic corrections to the density profile become important only at distances $x_+(t) - x \gtrsim w/[t_S \Gamma(k^m)]$ away from the tip of the shock wave, illustrated in Fig. 4. We find that the corrections to the shape are small at $x_+(t) - x \ll w/\Gamma(k^m)t_S$, albeit the density of fermions residing in the shock wave is suppressed by the factor $e^{-t \Gamma(k^m)}$.

In disregarding quantum ripples, the main result of Eq. (38) takes the zero-temperature fermionic distribution function to be either zero or one. As the region where the quantum dispersion is important grows linearly with time, it eventually encroaches on the scale where relaxation is significant, namely, $w/\Gamma(k^m)t_S$. It is meaningless to make claims on the modified shape of the classical profile once quantum ripples have encroached upon this region. The length scale for ripples and the length scale for kinematic corrections are comparable for $t \Gamma(k^m) \sim (\Delta N)^{2/3}$. This timescale therefore determines when Eq. (38) is no longer legitimate, as quantum corrections are important. Until this time, however, the main result of Eq. (38) holds: the shape of the shock is modified and subject to exponential decay of the magnitude with rate $\Gamma(k^m)$. We note that by the time $t \sim (\Delta N)^{2/3}/\Gamma(k^m)$ at which the “quantum” distortion meets with the “kinetic” one, destroying the shape as described by Eq. (38), its amplitude becomes exponentially small in the large parameter $(\Delta N)^{2/3}$ of the semiclassical theory.

A priori it is not clear how interactions should modify a shock wave. We have provided a picture motivated by a Boltzmann equation, where we explicitly determine the shape of the propagating shock at times well after the

formation of the shock, including generic interactions. Although $\Gamma(k^m)$ is given by a perturbative evaluation of Fermi’s golden rule for generic density-density interactions between spinless fermions [15], the strong momentum dependence of \mathcal{W} in Eq. (24) is a consequence of the limited phase space for scattering, which remains true even in the case of spinful fermions. We conjecture that our observations should be quite generic, as the form of $F(z)$ in Eq. (37) is not sensitive to the precise details of the rate \mathcal{W} . The main result of Eq. (36) exhibits the corrections to the naïve picture of a kinematic shock with exponential decay.

It remains of interest to investigate if there is a direct connection with the nonlinear Luttinger liquid [16] picture, in order to investigate this question in a more general, nonperturbative context [17].

ACKNOWLEDGMENTS

We acknowledge support from the Yale Postdoctoral Prize Fellowship (T.V.) and NSF DMR Grant No. 1603243 (L.G.).

APPENDIX A: EVALUATING THE BULK PROFILE

The approach we take to understand the time-evolved behavior of Eq. (10) for times $t \gg t_S$ is to consider a quadratic profile

$$k_F(x) = \begin{cases} k^m - (k^m - k^0)\left(\frac{x}{w}\right)^2, & |x| < w \\ k^0, & |x| \geq w. \end{cases} \quad (\text{A1})$$

When focusing on the front of the shock only the curvature at the maximum of the initial density perturbation should be important. The time evolution of the Wigner function is given by $x \rightarrow x - \frac{\hbar kt}{m}$, and at fixed x, t the roots of $k_F(x - \frac{kt}{m}) - k$ determine the upper and lower boundaries of support of the overhanging section of classical Wigner function. The case of Eq. (A1) causes these to be the roots of a quadratic polynomial

$$k_F\left(x - \frac{kt}{m}\right) - k = -(k^m - k^0)\tau^2(\kappa - \kappa_+)(\kappa - \kappa_-), \quad (\text{A2})$$

where

$$\kappa \equiv \frac{k^m - k}{k^m - k^0}, \quad \kappa_{\pm} = \lambda \pm \frac{\sqrt{\lambda}}{\tau}, \quad \tau \equiv \frac{t}{t_S}. \quad (\text{A3})$$

Here, we have assumed that $\lambda \gg \frac{1}{\tau}$. To evaluate the density we must plug the time-evolved equation (10) into Eq. (4). We wish to evaluate the excess density, defined as

$$\delta\rho(x, t) = \langle \Psi | \rho(x, t) | \Psi \rangle - \langle 0 | \rho(x, t) | 0 \rangle. \quad (\text{A4})$$

For the quadratic profile, this is equivalent to restricting the k integration of Eq. (4) to the region for which $|x - \frac{kt}{m}| \leq w$. In the new variables of Eq. (A3) this corresponds to

$$\lambda - \frac{1}{\tau} \leq \kappa \leq \lambda + \frac{1}{\tau}. \quad (\text{A5})$$

This window is sufficiently large to capture smearing of the Wigner function in the k direction even for nonquadratic profiles. Integrating κ between the bounds of Eq. (A5) yields

$$\delta\rho[\lambda, t] = (k^m - k^0) \int_{\lambda - \frac{1}{\tau}}^{\lambda + \frac{1}{\tau}} \frac{d\kappa}{2\pi} \int \frac{dy}{2\pi i(y + i0^+)} e^{iy(k^m - k^0)\tau^2(\frac{\kappa}{\tau^2} - (\kappa - \lambda)^2) - \frac{iy^3}{12} \frac{k^m - k^0}{w^2}}. \quad (\text{A6})$$

Rewriting the quadratic polynomial explicitly as in Eq. (A2), and introducing $y' \equiv y(\frac{k^m - k^0}{4w^2})^{1/3}$ and $\kappa' \equiv \kappa - \lambda$, gives

$$\delta\rho[\lambda, t] = (k^m - k^0) \int_{-\frac{1}{\tau}}^{\frac{1}{\tau}} \frac{d\kappa'}{2\pi} \int \frac{dy'}{2\pi i(y' + i0^+)} e^{-iy'(\Delta N)^{2/3}\tau^2(\kappa' - \kappa_+ + \lambda)(\kappa' - \kappa_- + \lambda) - iy'^3/3}, \quad (\text{A7})$$

where we have identified $\Delta N = 2w(k^m - k^0)$. We may now examine the $\tau \rightarrow \infty$ behavior of Eq. (A7). Up to a prefactor, this is in fact a function of one variable, $\lambda/\lambda_{\text{cr}}$, where

$$\lambda_{\text{cr}} = \frac{1}{(\Delta N)^{2/3}}. \quad (\text{A8})$$

This may be seen by defining $p \equiv \kappa' \tau (\Delta N)^{1/3}$, using the expressions for κ_{\pm} from Eq. (A3), and extending the range of the p integration to infinity to find

$$\delta\rho[\lambda, t] = (k^m - k^0) \int_{-\infty}^{\infty} \frac{dp}{2\pi \tau (\Delta N)^{1/3}} \int \frac{dy'}{2\pi i(y' + i0^+)} e^{-iy'(p^2 - \lambda/\lambda_{\text{cr}}) - iy'^3/3}. \quad (\text{A9})$$

Taking spatial derivatives of Eq. (A9), and making the substitutions (assuming $\lambda > 0$)

$$y = \frac{1}{2}(u - v)\sqrt{\frac{\lambda}{\lambda_{\text{cr}}}}, \quad p = \frac{1}{2}(u + v)\sqrt{\frac{\lambda}{\lambda_{\text{cr}}}}, \quad (\text{A10})$$

gives the form

$$\partial_x \rho[\lambda, t] = (k^m - k^0) \frac{\lambda}{2\lambda_{\text{cr}}} \frac{(\Delta N)^{1/3}}{w\tau^2} \left| \int \frac{du}{2\pi} e^{\frac{i}{2}(\lambda/\lambda_{\text{cr}})^{3/2}[u - u^3/3]} \right|^2, \quad (\text{A11})$$

which is valid at any $\lambda/\lambda_{\text{cr}}$. Using the definitions of λ , λ_{cr} , τ , $\ell(t)$ [of Eq. (12)], and ΔN , this is equivalent to Eq. (11). The leading asymptote for $\lambda/\lambda_{\text{cr}} \gg 1$ is

$$\delta\rho[\lambda, t] \approx (k^m - k^0) \left[\frac{\sqrt{\lambda}}{\pi \tau} + \frac{\sin\left(\frac{2}{3}(\Delta N)\lambda^{3/2}\right)}{2\pi \tau \lambda \Delta N} \right]. \quad (\text{A12})$$

APPENDIX B: DETERMINING CORRECTIONS IN LOW-ENERGY REGION

We begin from the expression for f_{low} of Eq. (33):

$$f_{\text{low}}[\lambda, \gamma, t] \approx 2c\Gamma(k^m)t_S e^{-t\Gamma(k^m)} [\gamma + \lambda]^{11/2} (1 - \gamma)^2 \int_0^{\lambda/\gamma} \frac{d\tau \sqrt{\tau}}{(1 + \tau)^{13/2}} e^{-\tau t \Gamma(k^m)\gamma}. \quad (\text{B1})$$

The contribution to the density, given by integrating over γ as in Eq. (35), relative to $\delta\rho_{\text{high}}$ is given by

$$\frac{\delta\rho_{\text{low}}[\lambda, t]}{\delta\rho_{\text{high}}[\lambda, t]} = \frac{c\Gamma(k^m)t}{\sqrt{\lambda}} \int_0^1 d\gamma [\gamma + \lambda]^{11/2} (1 - \gamma)^2 \int_0^{\lambda/\gamma} \frac{d\tau \sqrt{\tau}}{(1 + \tau)^{13/2}} e^{-\tau t \Gamma(k^m)\gamma}. \quad (\text{B2})$$

We will show that this integral is dominated by $\gamma \sim \mathcal{O}(1)$. In this case, we may approximate Eq. (B2) by setting $\lambda = 0$ in the lower integration limit and in $[\gamma + \lambda]^{11/2}$, and dropping the $(1 + \tau)^{13/2}$ denominator, which will be $1 + \mathcal{O}(\lambda)$. This then yields the simpler expression

$$\frac{\delta\rho_{\text{low}}[\lambda, t]}{\delta\rho_{\text{high}}[\lambda, t]} \approx \frac{c\Gamma(k^m)t}{\sqrt{\lambda}} \int_0^1 d\gamma \gamma^{11/2} (1 - \gamma)^2 \int_0^{\lambda/\gamma} d\tau \sqrt{\tau} e^{-\tau t \Gamma(k^m)\gamma}. \quad (\text{B3})$$

Equation (B3) depends only on the parameter $\lambda t \Gamma(k^m)$, and may be simply rewritten as

$$\frac{\delta\rho_{\text{low}}[\lambda, t]}{\delta\rho_{\text{high}}[\lambda, t]} \approx F(\lambda t \Gamma(k^m)), \quad F(z) = \frac{8}{5\sqrt{z}} \int_0^z dy \sqrt{y} e^{-y}. \quad (\text{B4})$$

We will now justify this procedure. First, we split the γ integral into two regions, focusing first on the region $\gamma < \lambda$:

$$I_1 \equiv \frac{c\Gamma(k^m)t}{\sqrt{\lambda}} \int_0^\lambda d\gamma [\gamma + \lambda]^{11/2} (1 - \gamma)^2 \int_0^{\lambda/\gamma} \frac{d\tau \sqrt{\tau}}{(1 + \tau)^{13/2}} e^{-\tau t \Gamma(k^m)\gamma}. \quad (\text{B5})$$

By changing integration variables it is clear that to leading order in λ this is given by

$$I_1 = \lambda^5 G(\lambda t \Gamma(k^m)), \quad G(k) \equiv ck \int_0^1 dx \int_0^1 dy \frac{\sqrt{y}(1+x)^{11/2} e^{-kx}}{(1+y/x)^{13/2} x^{3/2}}, \quad (\text{B6})$$

where $G(k) \sim k$ for $k \ll 1$, and is bounded by a constant for all $k > 0$. Turning now to the region $\gamma > \lambda$,

$$I_2 \equiv \frac{c\Gamma(k^m)t}{\sqrt{\lambda}} \int_\lambda^1 d\gamma [\gamma + \lambda]^{11/2} (1 - \gamma)^2 \int_0^{\lambda/\gamma} \frac{d\tau \sqrt{\tau}}{(1 + \tau)^{13/2}} e^{-\tau t \Gamma(k^m)\gamma}. \quad (\text{B7})$$

It is helpful to introduce the change of variables $z \equiv \tau t \Gamma(k^m)\gamma$, and explicitly include c from Eq. (24), such that

$$I_2 = \frac{168}{\sqrt{\lambda t \Gamma(k^m)}} \int_\lambda^1 d\gamma \frac{[\gamma + \lambda]^{11/2}}{\gamma^{3/2}} (1 - \gamma)^2 \int_0^{\lambda t \Gamma(k^m)} \frac{dz \sqrt{z}}{(1 + \frac{z}{\Gamma(k^m)\gamma})^{13/2}} e^{-z}. \quad (\text{B8})$$

The leading behavior in λ is given by setting $\lambda = 0$ in both the fractional power term and the lower limit of the γ integral, as well as discarding the denominator in the τ integral, giving

$$I_2 = F(\lambda t \Gamma(k^m)) + \mathcal{O}(\lambda), \quad (\text{B9})$$

with $F(z)$ given by Eq. (B4). The scale for I_1 to be comparable to I_2 is $\Gamma t \lambda \sim \lambda^{-10}$. For decay to be significant we require $\Gamma(k^m)t \gtrsim 1$, and as $\lambda \ll 1$ we are justified in considering only the contribution from I_2 . Putting all this together allows us to write the leading contribution as

$$\delta\rho_{\text{low}}[\lambda, t] = F(\lambda t \Gamma(k^m)) \delta\rho_{\text{high}}[\lambda, t], \quad (\text{B10})$$

with $\delta\rho_{\text{high}}[\lambda, t]$ given by Eq. (34). We note that the form of \mathcal{W} determines the particular numerical coefficients and powers appearing in the above expressions, but the form of the integral of F is insensitive to this. Indeed, the factors of $1/(1 + \tau)$ we neglect in the integrand of Eq. (B7) come from the $(k - p)$ dependence of \mathcal{W} in Eq. (24). This dependence arises from a combination of matrix elements and density of states of low-energy excitations. The density of states is small even in the presence of spin, and so it is possible that the form of F survives even in the case of weakly interacting spin- $\frac{1}{2}$ fermions.

APPENDIX C: CONSISTENCY OF APPROXIMATION

We wish to understand if the assumption of Eq. (21) is consistent. In order for this to be the case, the contribution to the source term from the low-energy region should be small compared to that of the high-energy region. This entails examining

$$\frac{J_{\text{low}}(x, k, t)}{J_{\text{high}}(x, k, t)} = \frac{\int_k^{k_-(x,t)} dp f(x, p, t) \mathcal{W}_{p \rightarrow k}}{\int_{k_-(x,t)}^{k_+(x,t)} dp f(x, p, t) \mathcal{W}_{p \rightarrow k}}. \quad (\text{C1})$$

We can rewrite this by using the expression for \mathcal{W} from Eq. (24), the dimensionless variable γ introduced in Eq. (32), and the same approximation for the denominator as in Eq. (25) to give

$$\frac{J_{\text{low}}[\lambda, \gamma, t]}{J_{\text{high}}[\lambda, \gamma, t]} = \frac{\int_0^\gamma d\gamma' f[\lambda, \gamma', t] (1 - \frac{\gamma'}{\gamma})^5}{2\sqrt{\lambda t} / t_S e^{-t \Gamma(k^m)}}. \quad (\text{C2})$$

By applying the same approximation technique as in Appendix B, one may obtain that the leading (in λ) relative correction to the source term is given by

$$\frac{J_{\text{low}}[\lambda, \gamma, t]}{J_{\text{high}}[\lambda, \gamma, t]} = \frac{\gamma^5}{165} (22 - 20\gamma + 5\gamma^2) F(\lambda t \Gamma(k^m)) + \mathcal{O}(\lambda), \quad (\text{C3})$$

where $F(z)$ is the same as in Eq. (B4). We observe that although the corrections are $\mathcal{O}(1)$ for $\lambda t \Gamma(k^m) \sim 1$, they are nonetheless numerically small, with the largest corrections being below 2%.

[1] G. B. Whitham, *Linear and Nonlinear Waves* (Wiley, Hoboken, NJ, 2011).

[2] I. V. Protopopov, D. B. Gutman, P. Schmitteckert, and A. D.

Mirlin, *Phys. Rev. B* **87**, 045112 (2013); I. V. Protopopov, D. B. Gutman, M. Oldenburg, and A. D. Mirlin, *ibid.* **89**, 161104(R) (2014).

- [3] A. G. Abanov and P. B. Wiegmann, *Phys. Rev. Lett.* **95**, 076402 (2005).
- [4] A. G. Abanov, E. Bettelheim, and P. Wiegmann, *J. Phys. A: Math. Theor.* **42**, 135201 (2009).
- [5] E. Bettelheim, A. G. Abanov, and P. Wiegmann, *Phys. Rev. Lett.* **97**, 246401 (2006); **97**, 161104(R) (2014).
- [6] E. Bettelheim and L. Glazman, *Phys. Rev. Lett.* **109**, 260602 (2012).
- [7] B. Bertini, M. Collura, J. De Nardis, and M. Fagotti, *Phys. Rev. Lett.* **117**, 207201 (2016).
- [8] B. Doyon and T. Yoshimura, *SciPost Phys.* **2**, 014 (2017).
- [9] B. Doyon, J. Dubail, R. Konik, and T. Yoshimura, *Phys. Rev. Lett.* **119**, 195301 (2017).
- [10] O. A. Castro-Alvaredo, B. Doyon, and T. Yoshimura, *Phys. Rev. X* **6**, 041065 (2016).
- [11] D. H. Cobden and B. A. Muzykantskii, *Phys. Rev. Lett.* **75**, 4274 (1995).
- [12] K. A. Matveev and A. Furusaki, *Phys. Rev. Lett.* **111**, 256401 (2013).
- [13] E. M. Lifshitz and L. P. Pitaevskii, *Statistical Physics, Part 2* (Elsevier, Oxford, 1980).
- [14] K. A. Matveev and Z. Ristivojevic, *Phys. Rev. B* **99**, 155428 (2019); W. DeGottardi and K. A. Matveev, *ibid.* **99**, 245121 (2019).
- [15] M. Khodas, M. Pustilnik, A. Kamenev, and L. I. Glazman, *Phys. Rev. B* **76**, 155402 (2007).
- [16] A. Imambekov, T. L. Schmidt, and L. I. Glazman, *Rev. Mod. Phys.* **84**, 1253 (2012).
- [17] E. G. Idrisov and T. L. Schmidt, *Phys. Rev. B* **100**, 165404 (2019).